Influence of the bending rigidity and the line tension on the mechanical stability of micropipette aspirated vesicles

Sovan Das*
Department of Mechanical Engineering, Indian Institute of Technology, Kanpur 208016, India
(Received 9 June 2010; revised manuscript received 9 July 2010; published 9 August 2010)

Micropipette aspiration technique can be very useful for describing the shape transitions of lipid bilayer vesicles with fluid phase coexistence modulated by the line tension and the bending rigidity. For example, composition dependence of the line tension at the liquid-ordered and liquid-disordered phase interface has been investigated using this technique. Recently, using a very simple mechanical model, the instabilities that occur during suction and release experiments of aspirated vesicles have been discussed. Due to its simplicity the model could not predict the influence of the bending rigidity. In this work, we incorporate the contributions from Helfrich bending energy and the line energy in the vesicle free energy and investigate the shape transitions in micropipette aspirated vesicles. We discuss how the critical aspiration pressure depends on the bending moduli of the phases, the line tension at the interface, and the reduced volume of the vesicle. The ratio of the bending moduli that we predict using the critical aspiration pressure data from recent experiments agrees with the literature.

DOI: 10.1103/PhysRevE.82.021908 PACS number(s): 87.16.D−, 82.70.Uv, 87.10.−e

I. INTRODUCTION

Lipid bilayer vesicles are formed when one or more types of lipid molecules are exposed to aqueous environment. The vesicles can have variety of shapes [1]. Theoretical models and analysis of different shapes and their transitions [2–5] were motivated by the early studies of red blood cells [6,7] and the discovery that the lipid bilayer membrane of a biological cell is a homogeneous fluid matrix with proteins embedded in it [8]. Subsequent finding that the membranes are inhomogeneous and patchy [9] led to development of experimental model systems of lipid bilayer vesicles with fluid phase coexistence [10–14]. Such experimental studies were also augmented by theoretical investigations of shapes and their transitions of lipid bilayer vesicles with fluid phase coexistence [15–19]. One of the key techniques employed to experimentally investigate shape transitions of red blood cells, liquid drops, and simple vesicles that preceded development of theories was micropipette aspiration. It has long been used to measure surface elastic, viscous, and thermoelastic properties of animal cells [6,7,20–26]. The technique has also been used in experimental studies of the formation of a tether, which is a membrane tube with diameter of few tens of nanometers, from a cell body or a vesicle [20,27–32]. In tether pulling experiments, on micropipette aspirated vesicles or cells, the aspirated part of the membrane acts as a material reservoir during tether formation and, as the length of the tether increases, the of length the vesicle inside the micropipette (projection length) decreases [30].

In earlier theoretical studies of aspirated vesicles, either the vesicle was assumed to have zero bending rigidity, or it was taken to be a flat infinite membrane with nonzero bending rigidity [21,22,30]. Without the bending rigidity, aspiration from a flat membrane gives a linear relationship between aspiration pressure and projection length [21,22]. This does not agree with experiments, unless, aspiration pressure is too large. Note that the analysis does not apply to bilayer vesicles directly because a nonzero shear modulus was considered in [21,22] whereas due to the assumption of fluid nature of the lipid bilayers shear modulus is zero. With bending rigidity a nonlinear relationship has been obtained, however, the analysis is only valid for thin discocytes and small pipette radius when compared to the size of the vesicle [21]. In the earlier experiments of the micropipette aspiration of cells or homogeneous vesicles the increment in the suction pressure were large (0.5–1 Pa) [33,34], and it was difficult to accurately resolve any instabilities in the process. Only recently, it has been possible to obtain small steps size increment (0.1 Pa) in the suction pressure. Hochmuth [24] theoretically observes, at the onset of aspiration, a liquid drop instability when the cell forms a hemispherical projection inside the pipette, i.e., the projection length equals the pipette radius. A similar instability has also been observed in the aspiration of two-phase vesicle which we describe in detail below.

Recently, there has been renewed interest in the application of micropipette techniques to lipid bilayer vesicles with liquid-ordered (l_o) and liquid-disordered (l_d) phase coexistence [35,36]. The technique has been used to apply a constant lateral tension in the experimental studies of sorting of lipids and proteins in membrane tethers [37–40]. The ability of the recent technique to apply suction pressure at small increments also made it possible to conduct experiments at low and controlled surface tension where bending rigidity plays a more important role. Tian *et al.* [35] have shown that the line tension at the domain interface can be directly measured as a function of the suction pressure and vesicle geometry by micropipette aspiration using a zero bending rigidity model for dumbbell shaped vesicles. Experimentally, they observed a critical aspiration pressure at the onset of aspiration. As the critical aspiration pressure is reached, the length of the vesicle aspirated into the pipette jumps to a large nonzero value within less than 1 s [35]. Moreover, they found

*sovandas@iitk.ac.in

that when the suction pressure is reduced from a large value, the projection length decreases and below a certain suction pressure the vesicle comes out of the pipette. This is the critical release pressure and the projection length corresponding to this pressure is the critical projection length. They also observed that the critical aspiration and release pressures are different, depending upon whether the l_o or the l_d domain is aspirated. Subsequently, Das *et al.* [36] considered a very simple mechanical model involving only the line energy as the vesicle free energy and discussed the instabilities observed in the experiments. The model ignored contribution from the nonzero bending rigidity to the free energy, and accordingly, it was applicable for vesicles deformed into limit shape of truncated spheres by large line tension [14]. The model in [36] was successful in describing the instabilities and the variation of suction pressure with projection length (length of aspirated vesicle inside the pipette) qualitatively. However, contrary to the experimental observations, the critical pressures in this model was independent of the aspirated phase. Furthermore, the influence of vesicle reduced volume, defined as

$$V_{red} = 3\hat{V}/(4\pi\hat{R}_0^3),$$

where the equivalent radius $\hat{R}_0$ is determined from the total surface area $\hat{A}$ of the vesicle membrane via

$$\hat{R}_0 = \sqrt{\hat{A}/4\pi},$$

was investigated. It was shown that the vesicles with reduced volume larger than a critical reduced volume for a given area fraction of the liquid-disordered phase are stable. The area fraction is defined as the ratio of the surface areas of the liquid-disordered phase and the entire vesicle. However, experimental data for reduced volume was not accurate enough to make the comparison.

In this work, we conduct a refined analysis of shape transitions of micropipette aspirated vesicles. We investigate the aspiration of single- and two-phase vesicles using a model that takes into account the elastic bending energy contribution to vesicle free energy. Here, we consider that the aspiration occurs from a vesicle, rather than an infinite flat membrane. This allows us to relax the assumption on the smallness of the pipette and shape of the vesicle to be aspirated considered in [21]. We discuss the influence of the bending rigidity, the line tension, and the reduced volume on the shape instabilities observed in micropipette aspirated vesicles. We first investigate the aspiration of a homogeneous (single phase) vesicle using the numerical solutions of the shape equations. We observe, contrary to the zero bending model, that the critical aspiration and release instabilities are present for all reduced volumes. Subsequently, we study the micropipette aspiration of a two-phase vesicle with nonzero bending rigidity. For the two-phase vesicle aspiration we focus on the aspiration instability only. We show that critical aspiration pressure depends significantly on the mechanical vesicle parameters such as bending rigidity of the phase that is aspirated and the line tension at the two-phase interface. We propose that the bending rigidity of the aspirated phase can be measured directly using the information about the experimental value of the critical aspiration pressure.

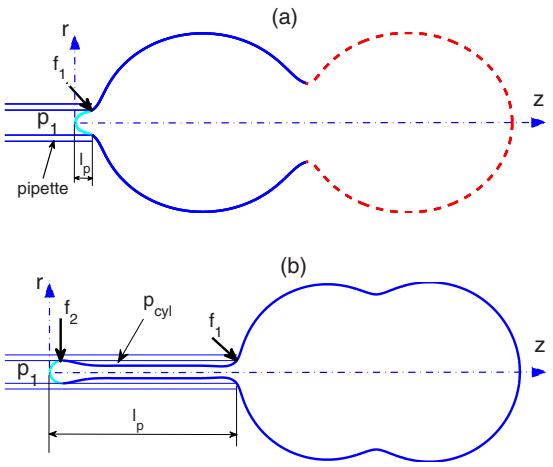

FIG. 1. (Color online) Schematic of aspirated vesicles. (a) A two-phase vesicle at the onset of aspiration when projection length is small (i.e., less than the pipette radius). f_1 is the normal force on the vesicle per unit circumferential length at the pipette mouth. (b) A single-phase vesicle after significant amount of vesicle is sucked into the pipette. f_2 is the normal force per unit length where the cap touches the pipette and p_{cyl} is the pressure in the gap between the pipette and the cylindrical region.

II. MODEL

In Fig. 1, we show the schematic of a two-phase axisymmetric vesicle that is aspirated within a micropipette of radius R_p. The experimental images of a few aspirated vesicles are shown in Fig. 2. The glass surface inside the pipette is assumed frictionless and the adhesion between the membrane and the micropipette has been omitted. Length of the vesicle inside the pipette (projection length) is denoted by l_p, ψ is the tangent angle measured from the r axis, and r is the distance of a point on the membrane from the axis of symmetry (z axis). Suction pressure p_1 and the vesicle pressure p are measured relative to the pressure outside of the vesicle

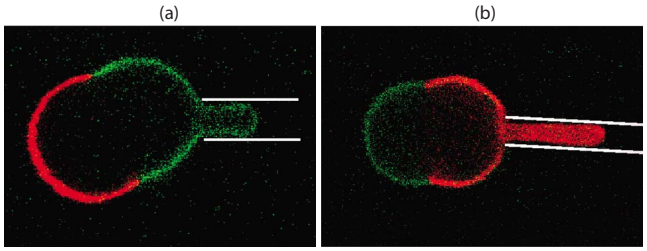

FIG. 2. (Color online) Experimental images of two-phase vesicles, that are axisymmetric, after aspiration. The images are obtained via a confocal microscope and correspond to the equatorial plane. (a) A vesicle with the l_o domain (green/thin) aspirated. The micropipette is schematically shown by two parallel lines. (b) A vesicle with the l_d domain (red/thick) aspirated. A gap between the membrane surface and the inside wall of the pipette is observed away from the aspirated tip.

and positive values of p indicate inner excess pressure. At the onset of aspiration, the projection length is small (l_p less than the pipette radius R_p), pipette touches the vesicle at the mouth only as shown in Fig. 1(a) and a force f_1 per unit length acts normal to the vesicle membrane, because the glass surface is assumed frictionless, at the pipette mouth.

Once significant amount of vesicle membrane is drawn inside the pipette a cylindrical region is formed as shown in Fig. 1(b). We assume that the membrane makes contact with the pipette at two locations, namely, at the end of the tube where a cap (aspirated tip) touches the pipette and at the pipette mouth. The normal forces at the two locations are f_2 and f_1, respectively. A gap between the cylindrical membrane region and the inner pipette wall is shown. The gap has also been seen in the experimental images of micropipette aspirated vesicles (see Fig. 2). We denote the pressure in this region, relative to the pressure outside of the vesicle, by p_{cyl}.

Through out the paper, we consider scaled quantities where lengths are made dimensionless by the equivalent radius $\hat{R}_0$ defined earlier, and forces are made dimensionless by the ratio of mean curvature bending rigidity κ_{ld} of the liquid-disordered phase and $\hat{R}_0$. We assume that during the course of the experiment the total surface area of the vesicle as well as the surface areas of individual phases are conserved. Accordingly, total surface area of the vesicle is 4π. From the equilibrium of the entire vesicle, along z direction, we obtain

$$f_1 = \frac{p_1}{2}\frac{R_p}{\cos\psi_p},$$

where f_1 is the force per unit length exerted by the pipette mouth on the vesicle and ψ_p is the tangent angle of the vesicle membrane at the pipette mouth. The values of ψ_p may be different for different vesicle shapes. The shape equations and jump conditions at the l_o–l_d interface are obtained by minimizing the energy functional with contributions from the total bending energy, the line energy at the interface, the pressure difference across the vesicle membrane at different regions (i.e., the cap and the cylindrical portion inside the pipette and the region outside the pipette) [5,15]. The shape equations and jump conditions can also be obtained by balancing the forces and moments on an infinitesimal area element of the membrane [20,32,41]. The detailed derivation of the shape equations are discussed in literature [5,15,18,20,32,41] and is not presented here. The differential equations for transverse shear stress Q_s and mean curvature h, for an axisymmetric membrane, are

$$(Q_s)' + (r'Q_s) + 2h(d - \varepsilon h^2) - 2\varepsilon h[2h(\sin\psi)/r + (\sin^2\psi)/r^2] + (p + p_i) = 0 \quad (1)$$

and

$$h' = -Q_s/\varepsilon. \quad (2)$$

In the above, the transverse shear stress per unit length Q_s acts perpendicular to the membrane surface and is different from the in-plane shear which is zero in the membrane due to its fluid nature. The prime denotes a derivative with respect to deformed arc length s; p is the dimensionless inner excess pressure inside the vesicle, d is a dimensionless constant associated with the determination of the mean lateral tension. The quantity p_i is different for different region. It is the suction pressure p_1 for the cap region, pressure p_{cyl} in the cylindrical region between the inner pipette surface and the vesicle surface of the tubular region inside the pipette, and zero outside the pipette. The parameter $\varepsilon \equiv \kappa_{lo}/\kappa_{ld}$ for the liquid-ordered phase, κ_{lo} being the bending rigidity of the liquid-ordered phase and $\varepsilon \equiv 1$ for the liquid-disordered phase. The assumption on the conservation of local surface area during deformation [4] relates deformed arclength s and the undeformed arclength S, which is the arclength parameter of a unit reference sphere, through the relation $(\cos S)' = -r$. The other differential equations needed to complete the system are $\psi' = -2h - (\sin\psi)/r$, $r' = \cos\psi$, and $z' = \sin\psi$. For the present study we ignore the effects of spontaneous curvature and Gaussian curvature rigidity. It has been shown in previous studies that these two parameters influence the location of the l_o–l_d phase boundary by a small amount [15,18,42] and they play important roles in discontinuous budding transitions [19]. In the present study vesicles shapes are significantly away from budding transitions and the spontaneous curvature and the Gaussian curvature rigidity should not play any important role in the aspiration and release instabilities.

The jump conditions for the transverse force, moment, and tangential force at the l_o–l_d interface, when the l_o phase is aspirated, are [18,15]

$$(Q_s)_{l_d} - (Q_s)_{l_o} = \sigma(\sin\psi^*)/r^*, \quad h_{l_d} - \varepsilon h_{l_o} = 0, \quad (3)$$

and

$$d_{l_d} - d_{l_o} - h_{l_d}^2 + \varepsilon h_{l_o}^2 = \sigma(\cos\psi^*)/r^*, \quad (4)$$

where σ is the line tension at the interface and ψ^* and r^* are, respectively, the tangent angle and radial distance at the interface. When the l_d phase is aspirated the first of jump condition 3 and the condition 4 are modified as

$$(Q_s)_{l_o} - (Q_s)_{l_d} = \sigma(\sin\psi^*)/r^*, \quad (5)$$

and

$$d_{l_o} - d_{l_d} - \varepsilon h_{l_o}^2 + h_{l_d}^2 = \sigma(\cos\psi^*)/r^*. \quad (6)$$

The variables ψ, r, and z are continuous across the interface. In the numerical solution strategy we consider cases in which only one phase (say, l_o) is inside the pipette and the l_o–l_d interface is always outside the pipette. Furthermore, we consider the domains outside and inside of the pipette as two separate regions with appropriate shape equations. To account for the force f_1 per unit length at the pipette mouth and impose that the vesicle touches the pipette we also need to apply the following conditions.

$$(Q_s)^{out} - (Q_s)^{in} = f_1 \quad \text{and} \quad r = R_p, \quad (7)$$

where the superscripts *out* and *in* denote the values just outside and inside of the pipette, respectively. The other variables are related through continuity across the pipette mouth. Once a significant amount of material is drawn inside the pipette and the cylindrical region forms as shown in Fig. 1(b), we need to specify the conditions at the junction be-

tween the aspirated tip and the cylinder. The transverse shear stresses at the junction are related by

$$(Q_s)^{cyl} - (Q_s)^{cap} = f_2. \tag{8}$$

The conditions $r=R_p$ and $\psi=\pi/2$ are imposed to ensure that the aspirated tip touches the pipette wall and to avoid the artificial penetration of membrane into the pipette wall. The other variables including r and ψ are continuous across the junction. Following [15,43] the shape equations and jump conditions can also be written in terms of the geometric quantities r and ψ. There is no significant advantage of using one approach over the other. However, the jump conditions are naturally expressed in terms of the jumps in forces and moments which is manifested in the present approach. The shape equations and jump conditions are obtained using the so called spontaneous curvature (SC) model for the curvature elasticity [2]. A more refined model, the area different elasticity (ADE) model, that takes into account the area difference between the monolayers and the stretching of individual monolayer areas [27,44,45] may also be employed. Furthermore, rapid displacement between the layers may take place during deformation resulting in a viscous drag at the bilayer midplane [20]. However, these models are most useful in the analysis of long tether formation and budding of vesicles, which involves regions of very high curvature and/or a rapid increase of curvature in the order of 1000-fold [20]. In the present mechanical stability analysis of the micropipette aspirated vesicles the ratio of the bilayer thickness to radius of curvature is in the range of 1/200 or less and such deformations are negligible and the effect of the area different elasticity has not been incorporated.

III. ASPIRATION OF A SINGLE-PHASE VESICLE

We first consider the aspiration of a single-phase vesicle. In the model, the two phases become indistinguishable if the bending moduli κ_{lo} and κ_{ld} are equal and there is no line tension acting at the l_o-l_d interface. Accordingly, in our numerical solution procedure, we choose $\varepsilon=1$ for the l_o phase and the line tension $\sigma=0$ for single-phase vesicle. We consider two scenarios shown in Figs. 1(a) and 1(b) separately. In the first scenario, the portion of the vesicle inside the pipette does not have the cylindrical region. In this scenario there are only two regions of the aspirated phase, namely, the region out side the pipette and the aspirated tip. In the second scenario, the portion inside the pipette consists of the aspirated tip and a cylindrical region connecting the tip with the region outside the pipette.

The first scenario posses a three-point boundary value problem (BVP) as boundary and jump conditions are applied where the tip touches the pipette, at the pipette mouth, and at the points where the vesicle intersects the z axis. In the second scenario we have a four-point BVP. In both the cases, we reparameterize the arclength to reduce the equations into two-point BVPs. The equations are then solved using MATLAB boundary value problem solver "*bvp4c*" with relative and absolute tolerance values of 10^{-6} and 10^{-8}, respectively. The force f_2 mentioned in Eq. (8) is an independent parameter, positive values of f_2 signify that a portion of the vesicle

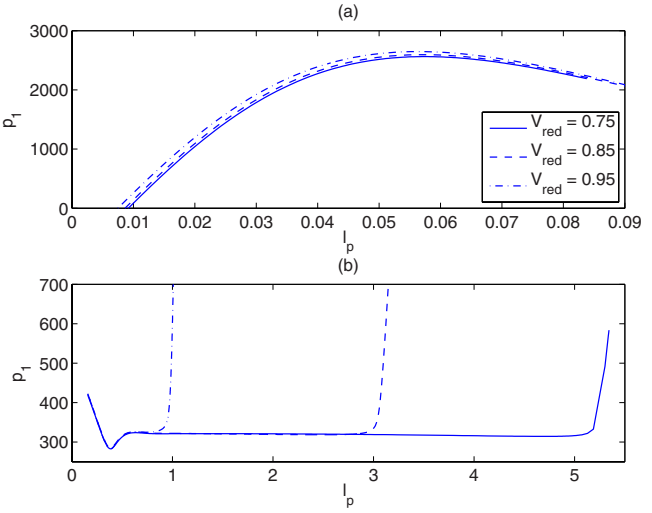

FIG. 3. (Color online) Variation of aspiration pressure with projection length for different reduced volumes for a single-phase vesicle and the pipette radius $R_p=0.1$. (a) At the onset of aspiration when l_p is small (first scenario). The maximum in each curve corresponds to the critical aspiration pressure p_{1cr}^{asp}. (b) For large projection length l_p (second scenario). The minimum corresponds to the critical release pressure p_{1cr}^{rel}. The values of critical pressures and their locations are provided in Table I. The critical pressures are not very sensitive to changes in reduced volume.

membrane inside the pipette is pressed against the pipette wall, whereas negative values are unphysical. The tip just touches the wall when $f_2=0$ along with the conditions on r and ψ mentioned previously. In the numerical solution, we assume $f_2=0$. This allows us to determine the pressure p_{cyl}. Furthermore, we find that, due to this condition, the membrane in the cylindrical region always stays within the pipette (i.e., the distance r of a point in the membrane within the pipette from z axis is less than the pipette radius R_p). It is also possible to determine p_{cyl} by fixing the volume between the membrane and the pipette, or specify $p_{cyl}=p_1$, or have p_{cyl} vary linearly from p_1 at the tip to 0 at the pipette mouth. However, when the projection length changes the volume also changes which precludes the first condition. In case of the other two we find that r is greater than R_p for one or more regions of the membrane inside the pipette, which is not physical. The first scenario allows the investigation of the critical aspiration, whereas in the second scenario, the pressure length curve for larger projection length is obtained and critical release has been observed.

Variation of p_1 with l_p is shown in Fig. 3 for different reduced volumes, for small and large projection lengths. For small projection lengths, in Fig. 3(a), a maximum is observed in the p_1-l_p curve. The maximum corresponds to the critical aspiration instability and the pressure is denoted as critical aspiration pressure p_{1cr}^{asp}. For large projection lengths (i.e., with the cylindrical region), in Fig. 3(b), the minimum in the p_1-l_p curve corresponds to the critical release instability and the pressure is denoted as critical release pressure p_{1cr}^{rel}. Note that the locations at which the critical aspiration instabilities occur are less than the pipette radius R_p, and they do not change significantly when the reduced volume and

TABLE I. Some exemplary values of the critical aspiration pressures (p_{1cr}^{asp}), critical release pressures (p_{1cr}^{rel}), and their locations for the aspiration of single-phase vesicles.

Red. vol.	p_{1cr}^{asp}	Location	p_{1cr}^{rel}	Location
0.75	2562.51	0.057	282.98	0.39
0.85	2595.20	0.057	285.16	0.38
0.95	2647.02	0.056	282.09	0.38

other parameters are varied (see Fig. 3 and Table I). The incorporation of the membrane bending rigidity into the model shows that the aspiration instability is different from the liquid drop instability predicted in Ref. [24].

Variation of suction pressure with projection length for large l_p, as shown in Fig. 3(b), is similar to that observed in Fig. 4c of Ref. [36] for the zero bending model for two-phase vesicles when the nonaspirated part is near spherical. However, the presence of the negative slope in the p_1-l_p plot for all the reduced volumes, along with the maxima in Fig. 3(a), imply that there is always a critical aspiration pressure (accordingly, an aspiration instability) at the onset of aspiration. Furthermore, the minimum in each of the p_1-l_p curve in Fig. 3(b) corresponds to the critical release instability and the pressure is denoted as critical release pressure p_{1cr}^{rel}. Note that the shape corresponding to reduced volume of 0.95 is almost spherical, yet the vesicle shows critical aspiration and release instabilities. These instabilities are also observed for $V_{red}=0.95$ in the case of two-phase vesicle aspiration. This value of the reduced volume has been found to be stable in the zero bending model [36].

IV. ASPIRATION OF A TWO-PHASE VESICLE

We now discuss the micropipette aspiration of two-phase vesicles. We focus on the onset of aspiration and the critical aspiration instability only. In this case, the system is defined by a four-point BVP which, like before, we reduce to a two-point BVP and numerically solve it using *bvp4c*. We keep the bending rigidity of the l_d phase fixed, then an increase in ε is equivalent to having an l_o phase with larger bending rigidity. In experiment this can be achieved by choosing different l_o lipid molecules in the ternary lipid mixture [12,13]. In Fig. 4, we show the variation of suction pressure p_1 with projection length l_p at the onset of aspiration, for two different values of ε, line tension σ, and reduced volumes. Existence of a maximum pressure in each plot, as in the case of the aspiration of a single-phase vesicle, ensures that there is a critical aspiration instability. The maximum suction pressure for $\varepsilon=5$ is approximately three times as large as the maximum suction pressure for $\varepsilon=1$, with other parameters kept fixed. The critical pressure also depends on the line tension which we discuss below. The changes in critical pressure is less significant when only the reduced volume is varied. The foregoing indicates that the bending rigidity may be the most important parameter in determining the critical aspiration pressure.

In Figs. 5(a) and 5(b), we present the variation of the critical pressure with ε, when the l_o phase ($(p_{1cr}^{asp})_{l_o}$) and the l_d phase ($(p_{1cr}^{asp})_{l_d}$) are aspirated, respectively, for different reduced volumes and two different line tension σ. We plot the variation of the ratio of the two critical aspiration pressures in Fig. 5(c). The changes in the vesicle reduced volume does not influence the critical pressures significantly. During the aspiration of the l_d phase, the l_o phase is away from the pipette mouth. In this case, we observe from Fig. 5(b) that

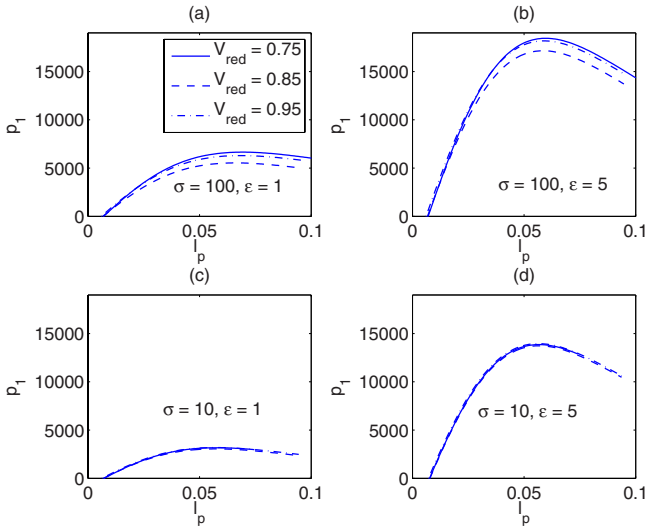

FIG. 4. (Color online) Variation of aspiration pressure with projection length in the first scenario for two-phase vesicle. The liquid ordered phase has been aspirated into the pipette. Pipette radius $R_p=0.1$ and the area fraction of the l_d phase $\chi=0.5$. The values of line tension σ and ε are as mentioned in the figure. Notice the difference in maximum p_1 values (critical aspiration pressures) for different values of ε and σ.

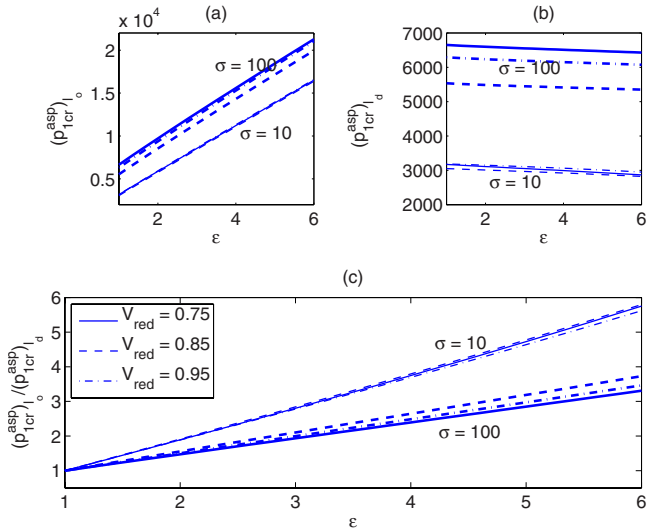

FIG. 5. (Color online) Variation of (a) critical aspiration pressure $(p_{1cr}^{asp})_{l_o}$ for the aspiration of l_o phase; (b) critical aspiration pressure $(p_{1cr}^{asp})_{l_d}$ for the aspiration of l_d phase; and (c) the ratio of the critical pressures $(p_{1cr}^{asp})_{l_o}/(p_{1cr}^{asp})_{l_d}$ with ε for different reduced volumes. Other parameters: $R_p=0.1$, $\chi=0.5$, $\sigma=10$ (thin lines), $\sigma=100$ (thick lines). The critical pressure $(p_{1cr}^{asp})_{l_d}$ does not change much with ε. The critical pressures and their ratio are almost insensitive to the vesicle reduced volume.

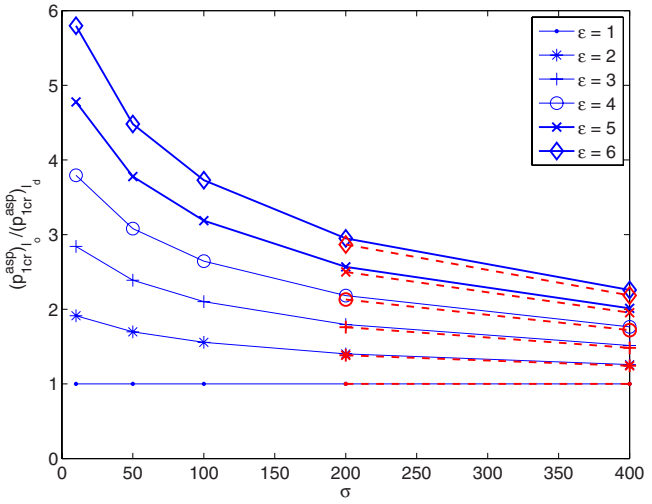

FIG. 6. (Color online) Variation of the ratio of the critical pressures $(p_1^{crit})_{l_o}/(p_1^{crit})_{l_d}$ with σ for different ε. The other parameters: R_p=0.1, V_{red}=0.85, χ=0.5 (solid lines), χ=0.4 (dashed lines). The critical pressures and their ratio are almost insensitive to the domain area fraction χ.

the sensitivity of critical aspiration pressure to increases in the bending rigidity of the l_o phase is low. Whereas the critical aspiration pressure during the aspiration of the l_o phase and the ratio of the critical pressures increase almost linearly with the bending rigidity of the l_o phase. In Fig. 6 we present the variation of the critical pressure ratio with the line tension σ for different values of ε. Notice that the range of change of the ratio with changes in σ is higher for larger values of ε. This was also indicated by the increasing gap between the thick (σ=100) and thin (σ=10) lines in Fig. 5. The exemplary values of the ratio of the bending rigidities and the line tension in Figs. 4 and 5 are chosen such that they cover a broad range and are of the same order in magnitudes with the observed values in literature [14,18,46].

We have also investigated the influence of the area fraction χ of the l_d phase and observed that χ does not play much of a role in determining the critical pressures (please see Fig. 6). Figures 5 and 6 together establish the fact that the geometric vesicle parameters such as reduced volume and domain area fraction do not play significant role in the quantification of the aspiration instability. An intuitive way of explaining such insensitivity is that at the critical aspiration instability it is necessary to induce a curvature at the pipette mouth in a direction opposite to that of the vesicle curvature. To a large extent this is local phenomena dominated by bending and the surface tension. A one-dimensional analog would be bending of a pretensioned beam. For small and moderate line tension considered here both the surface tension and its dependence on the reduced volume are small and bending dominates the critical aspiration instability. Furthermore, the area fraction determines the location of the phase boundary which is far enough from the pipette mouth to have any influence on the instability. These observations will not be valid if the line tension is large enough to induce a surface tension that is significantly higher than the bending energy and/or if the area fraction is such that the phase boundary is close to the pipette mouth. In the former scenario the predictions of zero bending model of Ref. [36] will hold. However, for the ranges of the line tension and the area fraction considered in the present study the critical aspiration pressures and their ratio depend sensitively on the bending rigidity and the line tension alone. This fact can be employed to measure these mechanical parameters accurately using the micropipette aspiration experiments which we briefly discuss below. Somewhat similar approach of estimating the bending rigidity of vesicle membranes via the critical suction pressure data, has been used by Zhelev *et al.* [33]. However, the aspiration technique involved holding the cell or single-phase vesicle by a large diameter pipette and deforming the membrane using a smaller diameter pipette. In the method described below only one micropipette has been used to deform a two-phase vesicle, and the accuracy of the measurement of the bending rigidity depends only on the critical aspiration data.

V. MEASUREMENT OF THE BENDING RIGIDITY

In [35], it was shown that the micropipette aspiration for two-phase vesicles can be effectively used to determine the line tension. The authors considered vesicles that were deformed into dumbbell shapes by the large line tension. In that case, the zero bending model could be used and the estimates of line tension varied from 0.5 to 3.3 pN depending on the composition of the ternary lipid mixture used to prepare the vesicles. Typical values of κ_{l_d} are of the order 10^{-19} J [47–49]. Experimental vesicles have sizes in the range 10 μm. Using these information we find that the dimensionless values of the line tension range from 50 to 330 which is well within the range we have considered in the present work. For the vesicles with molar composition of 0.34:0.28:0.38 (DOPC:Chol:ESM) Tian *et al.* [35] obtained the ratio of the critical aspiration pressures for the aspiration of l_o and l_d phases as 2.5 ± 0.23. The average line tension for the same composition is 1.3pN (see Fig. 3 of Ref. [35]). When made dimensionless the line tension becomes σ=130. Using the above information and from Fig. 6 we find that ε should be 4 ± 0.4. This value is close to earlier measurements [18,46]. The suction pressure in the experiments can be measured with an accuracy of 0.1–0.2 Pa [35,36] (error is less than 5%). Accordingly, an accurate and direct measurement of ε (hence the bending rigidity of the l_o phase) is possible using the micropipette aspiration technique. Furthermore, the present method provides an alternative to the existing methods [18,46]. It does not require fitting of vesicle shapes and, hence, the error introduced by fitting procedure is eliminated. *A priori* knowledge of line tension is needed for such measurements, which can be obtained using the methods proposed in Ref. [35] for large line tension. The line tension is calculated from the suction pressure and the geometric parameters at the phase boundary. For smaller line tension the method of [35] would not be accurate. In that case, estimate of the line tension can be obtained from the thermal fluctuation measurements of the phase interface [50].

Note that in the present work the slope (or, the tangent angle) has been assumed continuous across the $l_o - l_d$ phase boundary and we have not considered the presence of the

contact angle or a slope discontinuity at the phase boundary. Recent theoretical studies [51,52] predict such discontinuity, which has been verified experimentally [53]. These studies also discuss the influence of the contact angle on the line tension at the domain boundary. A modification of the shape equations and the formulation in the method presented here is required to incorporate such effects. Another limitation of the proposed method is that the line tension is provided as an input as discussed above. However, the method can be extended to estimate the line tension and the bending rigidity along with the contact angle at the domain boundary. The critical aspiration pressure data for the aspiration of the l_o and l_d for a large number of two–phase vesicles with different composition are required from experiments for such estimation. These enhancements will be discussed in future work.

VI. DISCUSSION

In this paper, we discuss micropipette aspiration of lipid bilayer vesicles with two fluid phases and study the influence of the mechanical and geometrical vesicle parameters on the instabilities observed during the aspiration. We find, by incorporating the bending rigidity in the model of micropipette aspiration, that critical aspiration and release instabilities are present, unlike the zero bending model, for all possible reduced volumes. We show, for the aspiration of a two-phase vesicle, that the critical suction pressure differs between the aspiration of the l_o and l_d phases. We observe that the ratio of the critical aspiration pressures depend on the mechanical vesicle parameters such as line tension and the bending rigidity of the aspirated phase. We also find that the ratio is not strongly influenced by the domain area fraction and the vesicle reduced volume. Furthermore, we present that the observations can be used to determine the mechanical parameters accurately via experimental measurements. The ratio of the bending moduli of the two phases determined using our method agrees with that published in the literature. Given that fact that the suction pressure can be measured with high accuracy and fitting of vesicle shapes is not necessary, the measurement of the mechanical parameters via the method presented here, will also be also very accurate.

ACKNOWLEDGMENTS

I am grateful to T. Baumgart for many stimulating discussions and for providing the experimental images of the aspirated vesicles. I would also like to thank J. T. Jenkins for helpful discussions.

[1] R. Lipowsky, Nature (London) **349**, 475 (1991).
[2] W. Helfrich, Z. Naturforsch **28c**, 693 (1973).
[3] H. J. Deuling and W. Helfrich, Biophys. J. **16**, 861 (1976).
[4] J. T. Jenkins, J. Math. Biol. **4**, 149 (1976).
[5] J. T. Jenkins, SIAM J. Appl. Math. **32**, 755 (1977).
[6] R. P. Rand, Biophys. J. **4**, 303 (1964).
[7] R. P. Rand and A. C. Burton, Biophys. J. **4**, 115 (1964).
[8] S. J. Singer and G. L. Nicholson, Science **175**, 720 (1972).
[9] D. M. Engelman, Nature (London) **438**, 578 (2005).
[10] C. Dietrich, L. A. Bagatolli, Z. N. Volovyk, N. L. Thompson, M. Levi, K. Jacobson, and E. Gratton, Biophys. J. **80**, 1417 (2001).
[11] S. L. Veatch and S. L. Keller, Phys. Rev. Lett. **89**, 268101 (2002).
[12] S. L. Veatch and S. L. Keller, Biochim. Biophys. Acta **1746**, 172 (2005).
[13] S. L. Veatch and S. L. Keller, Biophys. J. **85**, 3074 (2003).
[14] T. Baumgart, S. T. Hess, and W. W. Webb, Nature (London) **425**, 821 (2003).
[15] F. Jülicher and R. Lipowsky, Phys. Rev. E **53**, 2670 (1996).
[16] F. Jülicher and R. Lipowsky, Phys. Rev. Lett. **70**, 2964 (1993).
[17] R. Lipowsky, J. Phys. II **2**, 1825 (1992).
[18] T. Baumgart, S. Das, W. W. Webb, and J. T. Jenkins, Biophys. J. **89**, 1067 (2005).
[19] S. L. Das, J. T. Jenkins, and T. Baumgart, EPL **86**, 48003 (2009).
[20] E. Evans and A. Yeung, Chem. Phys. Lipids **73**, 39 (1994).
[21] E. A. Evans, Biophys. J. **13**, 941 (1973).
[22] E. A. Evans, Biophys. J. **30**, 265 (1980).
[23] E. A. Evans and A. Yeung, Biophys. J. **56**, 151 (1989).
[24] R. M. Hochmuth, J. Biomech. **33**, 15 (2000).
[25] R. Waugh and E. A. Evans, Biophys. J. **26**, 115 (1979).
[26] A. Yeung and E. A. Evans, Biophys. J. **56**, 139 (1989).
[27] B. Bozic, S. Svetina, B. Žekš, and R. E. Waugh, Biophys. J. **61**, 963 (1992).
[28] D. J. Bukman, J. H. Yao, and M. Wortis, Phys. Rev. E **54**, 5463 (1996).
[29] I. Derényi, F. Jülicher, and J. Prost, Phys. Rev. Lett. **88**, 238101 (2002).
[30] R. M. Hochmuth and E. A. Evans, Biophys. J. **39**, 71 (1982).
[31] D. C. Pamplona, J. A. Greenwood, and C. R. Calladine, J. Biomech. Eng. **127**, 1062 (2005).
[32] T. R. Powers, G. Huber, and R. E. Goldstein, Phys. Rev. E **65**, 041901 (2002).
[33] D. V. Zhelev, D. Needham, and R. M. Hochmuth, Biophys. J. **67**, 720 (1994).
[34] D. V. Zhelev, D. Needham, and R. M. Hochmuth, Biophys. J. **67**, 696 (1994).
[35] A. Tian, C. Johnson, W. Wang, and T. Baumgart, Phys. Rev. Lett. **98**, 208102 (2007).
[36] S. Das, A. Tian, and T. Baumgart, J. Phys. Chem. B **112**, 11625 (2008).
[37] A. Tian and T. Baumgart, Biophys. J. **96**, 2676 (2009).
[38] A. Tian, B. R. Capraro, C. Esposito, and T. Baumgart, Biophys. J. **97**, 1636 (2009).
[39] B. Sorre, A. Callan-Jones, J.-B. Manneville, P. Nassoy, J.-F. Joanny, J. Frost, B. Goud, and P. Bassereau, Proc. Natl. Acad. Sci. U.S.A. **106**, 5622 (2009).
[40] M. Heinrich, A. Tian, C. Esposito, and T. Baumgart, Proc. Natl. Acad. Sci. U.S.A. **107**, 7208 (2010).

[41] C. R. Calladine and J. A. Greenwood, J. Biomech. Eng. **124**, 576 (2002).
[42] S. L. Das and J. T. Jenkins, J. Fluid Mech. **597**, 429 (2008).
[43] J.-M. Allain and M. BenAmar, Eur. Phys. J. E **20**, 409 (2006).
[44] L. Miao, U. Seifert, M. Wortis, and H.-G. Döbereiner, Phys. Rev. E **49**, 5389 (1994).
[45] W. Wiese, W. Harbich, and W. Helfrich, J. Phys.: Condens. Matter **4**, 1647 (1992).
[46] S. Semrau, T. Idema, L. Holtzer, T. Schmidt, and C. Storm, Phys. Rev. Lett. **100**, 088101 (2008).
[47] H. P. Duwe, J. Käs, and E. Sackmann, J. Phys. (Paris) **51**, 945 (1990).
[48] E. A. Evans and W. Rawicz, Phys. Rev. Lett. **64**, 2094 (1990).
[49] V. A. Harmandaris and M. Deserno, J. Chem. Phys. **125**, 204905 (2006).
[50] C. Esposito, A. Tian, S. Melamed, C. Johnson, S.-Y. Tee, and T. Baumgart, Biophys. J. **93**, 3169 (2007).
[51] J.-B. Fournier and M. B. Amar, Eur. Phys. J. E **21**, 11 (2006).
[52] K. B. Towles and N. Dan, Biochim. Biophys. Acta **1778**, 1190 (2008).
[53] B. Božič and J. Majhenc, ChemPhysChem **10**, 2862 (2009).